Clays and Clay Minerals, Vol. 37, No. 4, 371–376, 1989.

EXPANDABLE SEPIOLITE FROM NINETYEAST RIDGE, INDIAN OCEAN

SCOTT ARGAST[1]

Department of Earth and Space Sciences
Indiana University–Purdue University at Fort Wayne
Fort Wayne, Indiana 46805

Abstract—The structure of sepiolite from a piston core obtained on Ninetyeast Ridge in the Indian Ocean was modified by exposure to ethylene glycol vapor. With ethylene glycol, the sepiolite 011 X-ray powder diffraction peak expanded from 12.4 to 12.8 Å, and the 130 peak contracted from 4.53 to about 4.45 Å. The cell modification is consistent with concomitant expansion along the *c*-axis and contraction along the *b*-axis. This structural distortion is not permanent, however, inasmuch as the sepiolite returned to its original state 6 to 12 hr after it was removed from the ethylene glycol-saturated atmosphere.

Key Words—Chemical composition, Ethylene glycol, Expansion, Sepiolite, X-ray powder diffraction.

INTRODUCTION

Sepiolite is a fibrous phyllosilicate consisting of three pyroxene-like chains extending parallel to the *a*-axis. These chains are joined to yield 2:1 phyllosilicate ribbons, which are linked by inversion of SiO_4 tetrahedra along adjacent edges. Discontinuities at the sites of inversion lead to the development of an open structure characterized by discontinuous octahedral sheets, continuous tetrahedral sheets, and structural channels oriented along the fiber axis (Figure 1).

The channels have approximate cross-sectional dimensions of 10.6 × 3.7 Å, giving sepiolite a large internal surface area of about 500 m^2/g (Serna and VanScoyoc, 1979). The large internal surface area explains many of sepiolite's properties, including its use as a molecular sieve and as a carrying agent for adsorbed molecules (see, e.g., Rausell-Colom and Serratosa, 1987). The small size of the channels restricts the free exchange of large nonpolar organic molecules, such as ethylene glycol, on the interior surfaces, although short-chain primary alcohols, such as methanol, ethanol, n-propanol, and n-butanol, can penetrate (Serna and VanScoyoc, 1979; Serratosa, 1979). Sepiolite is not generally regarded as an expandable mineral, but several occurrences of expandable sepiolite have been reported. Güven and Carney (1979), for example, reported expansion from 12.14 to 12.28 Å with the addition of ethylene glycol. A sepiolite sample from marine sediments in the Santa Cruz basin was found by Fleischer (1972) to expand with the addition of glycerol, and Jones and Galan (1988) reported a specimen expandable with dimethylsulfoxide.

Palygorskite is a related fibrous phyllosilicate, which differs from sepiolite in details of structure, chemistry, and size of the channels. Palygorskite contains more Al and less Mg than sepiolite and, because it contains only two pyroxene-like chains, the dimensions of the channels are only 3.7 × 6.4 Å (Ovcharenko, 1964). Like sepiolite, the size of palygorskite's channel restricts the free adsorption of large nonpolar organic molecules. Recently, however, Jeffers and Reynolds (1987) described a palygorskite from the Mangyshlak Peninsula, Soviet Union, which freely adsorbed and expanded with ethylene glycol. Jeffers and Reynolds (1987) ascribed this expandability to the size of the 002 spacing and to the strength of bonds between adjoining 2:1 ribbons for this particular palygorskite.[2]

In the present paper, sepiolite from a deep-sea piston core obtained on Ninetyeast Ridge in the Indian Ocean is described. This sample expanded in the presence of ethylene glycol, and its expansion behavior is evaluated in terms of the internal dimensions of the structural channels.

EXPERIMENTAL

Materials

The samples were obtained from Lamont-Doherty piston core Vema 34-61. The piston core was obtained in 4397 m of water on the west flank of Ninetyeast Ridge, Indian Ocean, at 5°51.5′S latitude and 88°29.5′E longitude (Figure 2). The sepiolite occurs as disseminated masses in a coccolith- and discoaster-bearing, clinoptilolite-sepiolite clay from about 7 to 32 cm sub-

[1] Correspondence to: Scott Argast, Department of Earth and Space Sciences, Indiana-Purdue University at Fort Wayne, 2101 Coliseum Blvd., East, Fort Wayne, IN 46805-1499.

[2] The fibrous phyllosilicates have customarily been indexed in the same manner as other orthorhombic crystals, in that $c < a < b$; however, it is becoming increasingly common to index them by the convention that $a < c < b$ (see, e.g., Jones and Galan, 1988). Although unorthodox, this convention makes the *c*-axis of sepiolite and palygorskite normal to the tetrahedral and octahedral layers. This convention will be used for new data reported here, and data from the literature will be transformed accordingly.

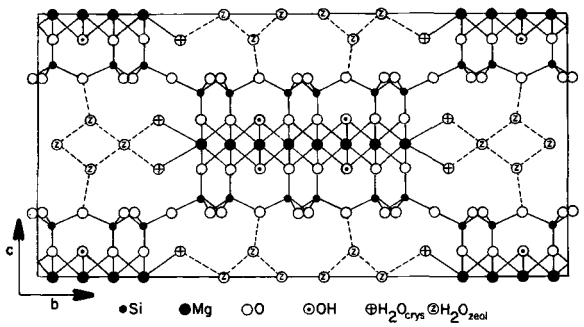

Figure 1. Projection on 100 of the sepiolite unit cell (after Brauner and Preisinger, 1956).

bottom depth and as a vein that cuts a coccolith-discoaster ooze from 100 to 128 cm subbottom depth. The discoasters are of Paleogene age, and because the sepiolite is disseminated and intimately mixed with the discoasters of the upper interval, the sepiolite is probably also of Paleogene age.

Methods

Twenty-three samples were obtained from the core. Smear slides of all samples were examined with the petrographic microscope, and selected samples were examined with the scanning electron microscope. Routine X-ray powder diffraction (XRD) patterns were made for all samples using a Philips APD 3520 system with an automatic theta-compensating slit, a graphite monochromator, Cu radiation, and a scan rate of 0.017°/s. Samples for XRD analysis were first dispersed in water, disaggregated with an ultrasonic processor, and settled onto glass slides, or on single-crystal quartz slides cut to minimize the quartz reflections. The ultrasonic disaggregation caused some gelling of the sepiolite-bearing samples.

After the initial XRD survey, sepiolite-bearing samples were selected from the intervals at 29-, 32-, 115-, and 117-cm subbottom depths. XRD patterns of these samples were obtained by step scanning at intervals of 0.005°2θ with measure times from 2.5 to 10 s per step. The step-scanned data were gathered electronically and smoothed using a 7-point moving average. These techniques significantly reduced noise and enhanced resolution.

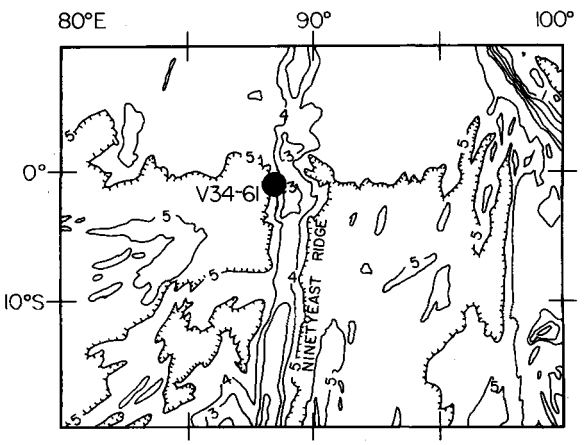

Figure 2. Location of piston core V34-61 on the west flank of Ninetyeast Ridge, Indian Ocean. Bathymetric contours are in kilometers.

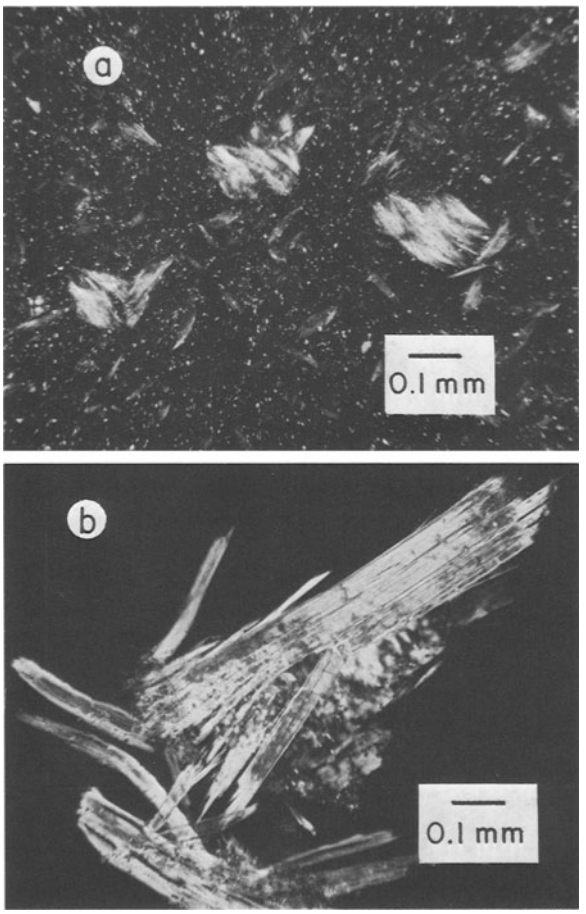

Figure 3. Photomicrographs of sepiolite from core V34-61, showing typical morphologies.

The V34-61 sepiolite generally expanded within 12 hr after exposure to ethylene glycol vapor, but samples were glycolated for at least 24 hr at 60°C to assure full effect. The expanded sepiolite began reverting to its unexpanded form 6 to 12 hr after it was removed from the ethylene glycol-saturated atmosphere. A tray of ethylene glycol was therefore placed in the sample chamber of the diffractometer to prevent reversion to the unexpanded form during lengthy step-scans.

The sepiolite could not be physically separated from either the calcareous ooze or the clinoptilolite, and an acid treatment to remove the ooze was not feasible because of sepiolite's sensitivity to low pH. The resultant calcite and clinoptilolite interfered with some

https://doi.org/10.1346/CCMN.1989.0370411 Published online by Cambridge University Press

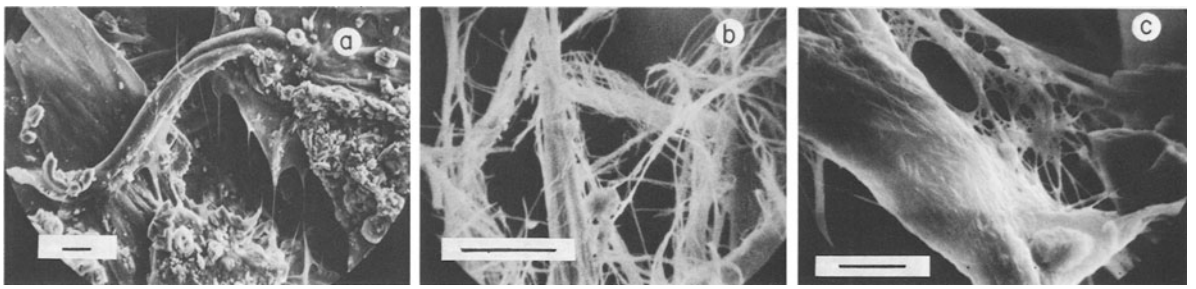

Figure 4. Scanning electron micrographs of sepiolite from core V34-61. Scale bars: (a) 10 μm; (b and c) 5 μm.

of the sepiolite XRD peaks, but provided useful internal standards after calibration to fluorite, halite, and/or silicon that was added to the samples.

RESULTS

Morphology

The vein sepiolite occurred as a mass of matted and interwoven fibers that formed a thin sheet having the consistency of coarse paper. The vein was not evident in the overlying nannofossil-bearing, clinoptilolite-sepiolite clay, but the sepiolite was highly visible in the upper interval as disseminated blebs of interwoven fibers, some as long as several millimeters.

Under the petrographic microscope, the sepiolite appears as laths and sheaf-like bundles of intertwined, length-slow fibers, typically 0.1 to 0.15 mm long, although larger bundles were noted (Figure 3). The characteristic fibrous morphology was also evident in scanning electron micrographs (Figure 4) and was similar to the feathery to fibrous morphology of sepiolite from other localities such as Valdemoro, Spain; Eskisehir, Turkey; and Two Crows, Nevada.

Chemistry

The chemical composition of the samples from the 28- and 117-cm levels was determined using the rapid wet methods of Shapiro (1975). The results, recast on an H_2O- and $CaCO_3$-free basis, are given in Table 1, along with the compositions of several other sepiolite samples reported in the literature.

The composition of the sepiolite from core V34-61 is similar to the composition of other sepiolite samples and to the predicted chemistry of an ideal sepiolite, according to the Brauner and Preisinger (1956) model. The vein sample at 117 cm differed slightly in composition from the disseminated sample at 28 cm, probably because the bulk samples contained material other than sepiolite. For example, the high concentration of P_2O_5 in the 28-cm sample is attributable to the abundant presence of fish teeth in the upper portions of the core, and the greater Al_2O_3, K_2O, and Na_2O of the 28-cm sample is well explained by the presence of clinoptilolite.

X-ray powder diffraction

X-ray powder diffraction (XRD) patterns for glycolated and unglycolated samples from the 29- and 117-cm intervals are shown in Figures 5 and 6. These samples are representative of the sepiolite from the upper and lower portions of the core. The V34-61 samples yielded XRD patterns typical of poorly crystalline sepiolite. The unglycolated samples were characterized by a strong reflection at about 7.1°2θ (011), a moderately strong reflection at about 19.6°2θ (130), and several other moderate to very weak reflections characteristic of sepiolite (Figures 5 and 6). Chlorite and clinoptilolite were abundant in the 29-cm sample, and calcite was abundant in the veined sample from 117 cm. A strong, broad, complex reflection was noted at about 27°2θ. Assignment of *hkl* values to this reflection was not possible, although the peak was probably a composite of quartz plus several sepiolite reflections.

Glycolation produced a strong expansion of the 011 peak from about 12.4 to 12.8 Å and a concomitant collapse of the 130 peak from about 4.53 to about 4.45 Å. The broad peak in the unindexed region at about

Table 1. Chemical compositions of some marine sepiolite samples.[1]

	1	2	3	4	5
SiO_2	63.5	67.0	68.09	72.	69.10
TiO_2	0.37	0.03	0.00	0.03	
Al_2O_3	8.6	1.1	0.52	0.65	
Fe_2O_3[2]	3.66	0.09	0.30	2.1	
MnO	0.59	0.00	0.00	0.05	
MgO	16.8	31.1	29.4	24.	30.90
Na_2O	1.18	0.23	1.37	0.93	
K_2O	1.79	0.27	0.13	0.0	
P_2O_5	3.48	0.14	0.15	0.0	

1. This study: Core V34-61, 28 cm. Bulk sample; contains clinoptilolite and fish teeth.
2. This study: Core V34-61, 117 cm. Picked sepiolite from vein.
3. Hathaway and Sachs (1965); Mid-Atlantic Ridge.
4. Fleischer (1972); Santa Cruz basin, California.
5. Brauner and Preisinger (1956); theoretical composition of ideal sepiolite.

[1] Analyses reported on an H_2O- and $CaCO_3$-free basis.
[2] Total iron as Fe_2O_3.

https://doi.org/10.1346/CCMN.1989.0370411 Published online by Cambridge University Press

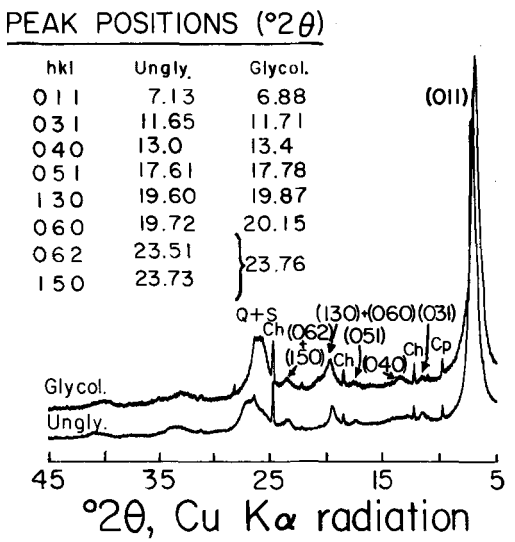

Figure 5. X-ray powder diffraction patterns of unglycolated and glycolated samples from core V34-61, 29 cm. Samples were oriented on a quartz slide cut perpendicular to the *c*-axis. Labelled *hkl* values are for sepiolite. Chlorite (Ch) and clinoptilolite (Cp) are also present. Sepiolite peaks at angles >25°2θ were too broad to index accurately. The peak labelled Q+S is probably a composite of sepiolite and a weak quartz reflection.

27°2θ also expanded substantially. Small collapses in the d-values of the 040, 051, and 060 XRD peaks were also observed.

As noted above, the sepiolite began to revert to its

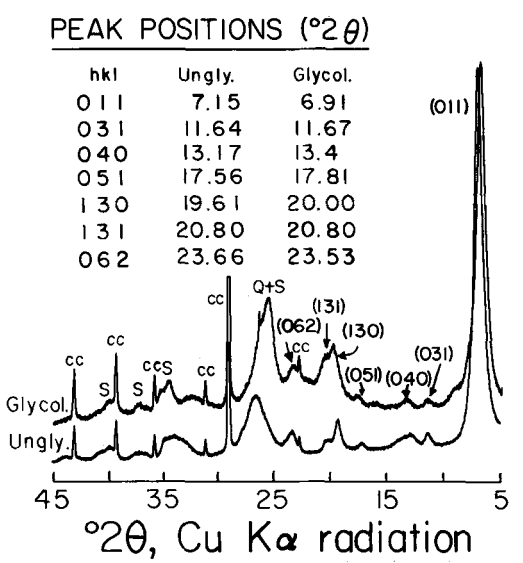

Figure 6. X-ray powder diffraction patterns of unglycolated and glycolated samples from core V34-61, 117 cm. Samples were oriented on a quartz slide cut perpendicular to the *c*-axis. Labelled *hkl* values are for sepiolite. Calcite (cc) is abundant. Several sepiolite peaks are labelled at 2θ >25°, but these were much too broad to index accurately. The peak labelled Q+S is probably a composite of sepiolite and a weak quartz reflection and shows strong expansion with the addition of ethylene glycol.

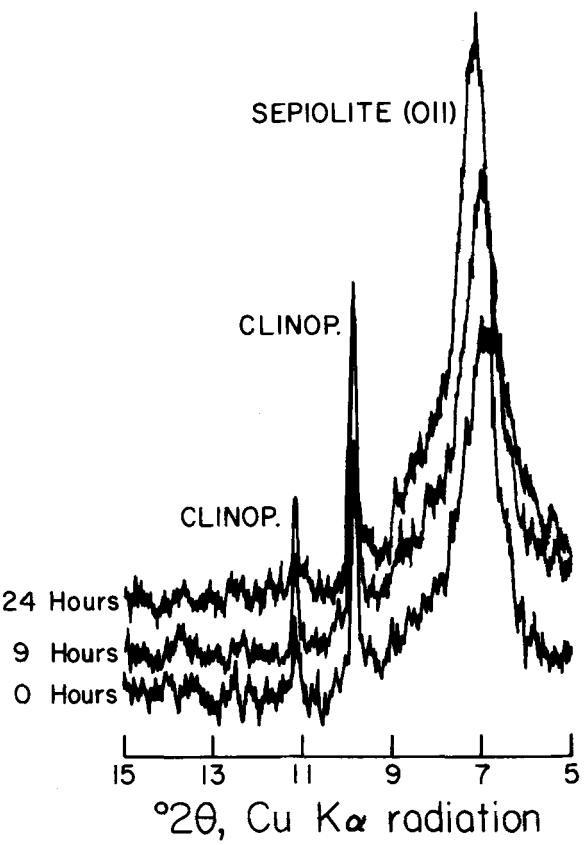

Figure 7. X-ray powder diffraction patterns of sepiolite and clinoptilolite from core V34-61, 29 cm. Patterns are shown at 0, 9, and 24 hr after removal from an ethylene glycol-saturated atmosphere. The sepiolite structure returned to its unglycolated state 6 to 12 hr after removal from the glycolator.

original state about 6–12 hr after it was removed from the ethylene glycol-saturated atmosphere. Figure 7 shows the sepiolite 011 reflection for the sample from the 29-cm interval in its fully glycolated state and 9 and 24 hr after removal from the glycolator. As the sample deglycolated, the 011 reflection collapsed to its original position. This process could be repeated, and no change was noted in the expansion-collapse behavior after as many as five glycolation-deglycolation cycles.

DISCUSSION

The XRD patterns were indexed to an orthorhombic cell in space group *pncn*, and cell parameters were refined using the NBS*AIDS83 program for crystal cell refinement (Tables 2 and 3; Mighell *et al.*, 1981). The poor crystallinity and broad reflections introduced uncertainty to the calculations, although the data gave relatively consistent estimates of the cell dimensions.

The calculated orthorhombic cell parameters for the air-dried sepiolite at 29 cm are a_o = 5.22, b_o = 27.05, and c_o = 13.94 Å; and for the sepiolite at 117 cm, a_o = 5.21, b_o = 27.00, and c_o = 13.83 Å. The cell parameters for the ethylene glycol-solvated sepiolite at 29 cm

https://doi.org/10.1346/CCMN.1989.0370411 Published online by Cambridge University Press

Table 2. Calculated and observed d-values (Å) for unglycolated and glycolated sepiolite from core V34-61, 29 cm.

	Air-dried		Ethylene glycol-solvated	
hkl	Obs	Calc[1]	Obs	Calc[2]
011	12.4	12.4	12.8	12.9
031	7.60	7.57	7.56	7.56
040	6.8	6.8	6.6	6.6
051	5.04	5.04	4.99	4.98
130	4.53	4.52	4.47	4.47
060	4.50	4.51	4.41	4.41
062	3.78	3.79	3.74	3.78
150	3.75	3.76		3.70

[1] a_o = 5.22, b_o = 27.05, c_o = 13.94 Å.
[2] a_o = 5.18, b_o = 26.46, c_o = 14.71 Å.

Table 3. Calculated and observed d-values (Å) for unglycolated and glycolated sepiolite from core V34-61, 117 cm.

	Air-dried		Ethylene glycol-solvated	
hkl	Obs	Calc[1]	Obs	Calc[2]
110	12.4	12.3	12.8	12.9
130	7.60	7.54	7.58	7.56
040	6.72	6.75	6.61	6.62
150	5.05	5.03	4.98	4.98
031	4.53	4.51	4.44	4.45
131	4.27	4.29	4.27	4.26
260	3.76	3.77	3.78	3.78

[1] a_o = 5.21, b_o = 27.00, c_o = 13.83 Å.
[2] a_o = 5.16, b_o = 26.46, c_o = 14.70 Å.

are a_o = 5.18, b_o = 26.46, and c_o = 14.71 Å; and for the sepiolite at 117 cm, a_o = 5.16, b_o = 26.46, and c_o = 14.70 Å. Air-dried sepiolite was reported by Nagata *et al.* (1974) to have a_o = 5.281, b_o = 26.88, and c_o = 13.43 Å, typical of values reported in the literature.

The width of the structural channel along the *c*-axis of sepiolite and palygorskite is usually about 3.7 Å. This is too narrow to permit access of the ~4-Å wide ethylene glycol molecule (Reynolds, 1965); however, the V34-61 sepiolite is unusual in that it is about 0.5 Å larger along *c* than most other sepiolite samples. This extra 0.5 Å provides a channel sufficiently large for entry of the ethylene glycol molecule. The situation is exactly analogous to the one described by Jeffers and Reynolds (1987) for expandable palygorskite. They found that a slightly larger than average *c*-axis dimension in palygorskite from the Mangyshlak Peninsula permitted entry of ethylene glycol and consequent expansion of the 011 XRD peak from 10.4 to 10.7 Å.

Along the *b*-axis the structural channel measures 10.6 Å in sepiolite and 6.4 Å in palygorskite. Neither of these are small enough to limit free access of ethylene glycol and present no limitation to the expansion behavior of either sepiolite or palygorskite (Jeffers and Reynolds, 1987).

Unlike smectite and other expandable phyllosilicates, sepiolite does not have continuous tetrahedral-octahedral layers. Instead, sepiolite presents discrete T–O–T strips diagonally attached to adjacent T–O–T strips through oxygen bonds (Figure 1). The presence of this bond limits the expansion that can occur along *c* without a consequent collapse along *b*, with or without an attendant twisting of the structure similar to the 'crystal-folding' that occurs during the high-temperature dehydration of sepiolite (see, e.g., Figure 1 in Serratosa, 1979). The calculated *b* parameter of the V34-61 sepiolite reflects this *b*-axis collapse. For example, b_o for the air-dried sepiolite from core V34-61 at 29 cm is 27.05 Å, and for its glycolated counterpart b_o is 26.46 Å. A similar collapse was noted for the sample from 117 cm.

Although they did not note it, the same collapse along the *b*-axis should have occurred in the expandable palygorskite examined by Jeffers and Reynolds (1987). Their failure to note a change in the *b*-axis dimension could have been due, however, to the presence of interfering peaks that masked the collapse.

Symmetry would be lost in going from the unfolded to the folded structure, but the data reported here do not permit discriminating between the two possibilities of simple collapse along *b*, or collapse accompanied by folding.

Golden *et al.* (1985) described the alteration of palygorskite and sepiolite to smectite under alkaline condition. They suggested that the alteration was by processes dominated by solution-reprecipitation, with simulataneous reorganization of the fibrous structure by the disruption of Si–O–Si bonds. The results from the study of the V34-61 sepiolite, especially the observed collapse on the *b*-axis and consequent structural distortion, indicate the possibility that the Si–O–Si bonds of the V34-61 sepiolite were stretched. This stretching could provide a mechanism for the structural transformation of the fibrous phyllosilicates as described by Golden *et al.* (1985), although further work with polar organic molecules is necessary to clarify the process (Jones and Galan, 1988).

ACKNOWLEDGMENTS

I thank K. M. Towe for providing a sample of sepiolite from Eskisehir, Turkey. Discussions with H. E. Roberson and reviews by R. C. Reynolds and E. Galan are gratefully acknowledged. Equipment support was provided by NSF grant CSI-8750250, and research support was provided by an IPFW Summer Grant for Research. Piston core samples were provided by Lamont-Doherty Geological Observatory through NSF grant OCE85-00232 and Office of Naval Research grant N00014-84-C-0132.

REFERENCES

Brauner, K. and Preisinger, A. (1956) Structure of sepiolite: *Mineral. Petrog. Mitt.* **6,** 120–140.
Fleischer, P. (1972) Sepiolite associated with Miocene di-

atomite, Santa Cruz basin, California: *Amer. Mineral.* **57,** 903–913.

Golden, D. C., Dixon, J. B., Shadfan, H., and Kippenberger, L. A. (1985) Palygorskite and sepiolite alteration to smectite under alkaline conditions: *Clays & Clay Minerals* **33,** 44–50.

Güven, N. and Carney, L. L. (1979) The hydrothermal transformation of sepiolite to stevensite and the effect of added chlorides and hydroxides: *Clays & Clay Minerals* **27,** 253–260.

Hathaway, J. C. and Sachs, P. L. (1965) Sepiolite and clinoptilolite from the Mid-Atlantic Ridge: *Amer. Mineral.* **50,** 852–867.

Jeffers, J. D. and Reynolds, R. C., Jr. (1987) Expandable palygorskite from the Cretaceous-Tertiary boundary, Mangyshlak Peninsula, U.S.S.R.: *Clays & Clay Minerals* **35,** 473–476.

Jones, B. F. and Galan, E. (1988) Sepiolite and palygorskite: in *Hydrous Phyllosilicates (Exclusive of Micas), Reviews in Mineralogy 19,* S. W. Bailey, ed., Mineralogical Society of America, 631–674.

Mighell, A. D., Hubbard, C. R., and Stalick, J. K. (1981) NBS*AIDS80: A FORTRAN program for crystallographic data evaluation: *Natl. Bur. Stand. Tech. Note* **1141,** 54 pp.

Nagata, H., Shimoda, S., and Sudo, T. (1974) On dehydration of bound water of sepiolite: *Clays & Clay Minerals* **22,** 285–293.

Ovcharenko, F. D. (1964) *The Colloid Chemistry of Palygorskite:* Israel Program for Scientific Translations, Jerusalem, 101 pp. (translated from Russian).

Rausell-Colom, J. A. and Serratosa, J. M. (1987) Reactions of clays with organic substances: in *Chemistry of Clays and Clay Minerals,* A. C. D. Newman, ed., Mineralogical Society, London, 371–422.

Reynolds, R. C., Jr. (1965) An X-ray study of the ethylene glycol-montmorillonite complex: *U.S. Army Cold Regions Res. Eng. Lab. Res. Rept.* **171,** 9 pp.

Serna, C. J. and VanScoyoc, G. E. (1979) Infrared study of sepiolite and palygorskite surfaces: in *Proc. Int. Clay Conf., Oxford, 1978,* M. M. Mortland and V. C. Farmer, eds., Elsevier, Amsterdam, 197–206.

Serratosa, J. M. (1979) Surface properties of fibrous clay minerals (palygorskite and sepiolite): in *Proc. Int. Clay Conf., Oxford, 1978,* M. M. Mortland and V. C. Farmer, eds., Elsevier, Amsterdam, 99–109.

Shapiro, L. (1975) Rapid analysis of silicate, carbonate and phosphate rocks—Revised edition: *U.S. Geol. Surv. Bull.* **1401,** 76 pp.

(Received 27 September 1988; accepted 4 February 1989; Ms. 1836)